Mining Security Assessment in an Underground Environment using a Novel Face Recognition Method with Improved Multiscale Neural Network

Xinhua Liu[1], Peng Qi[1], Patrick Siarry[2], Dezheng Hua[1], Z. Ma[3], Xiaoqiang Guo[1], Orest Kochan[4], Z. Li[5*]

1. School of Mechatronic Engineering, China University of Mining and Technology, Xuzhou, China
2. University Paris-Est Créteil Val de Marne, 61 Av. du General de Gaulle, 94010, Creteil, France
3. Sustainable Buildings Research Centre, University of Wollongong, 2522, Australia
4. Department of Telecommunications, Lviv Polytechnic National University, Bandery 12, 79013 Lviv, Ukraine
5. Faculty of Mechanical Engineering, Opole University of Technology, 45-758 Opole, Poland

* Corresponding author.

Abstract: Overstaffing production in underground coal mining is not convenient for daily management, and incomplete information of coal miners hinders the rescue process of firefighters during mine accidents. To address this safety sustainability issue, a novel face recognition method based on an improved multiscale neural network is proposed in this paper. A new depthwise seperable (DS)-inception block is designed and a joint supervised loss function based on center loss theory is developed to constructe a new multiscale model. The miniers can be recognized in the harsh underground environment during the life rescue. Experimental results show that the accuracy, recall and F1-score indexes of the proposed method for the miner face recognition in the underground mining environment are 97.26%, 94.17% and 95.42%, respectively. Transfer model with joint supervised loss can effectively improve the recognition accuracy by about 0.5~1.5%. In addition, the average recognition accuracy of the proposed face recognition method achieves to 91.34% and the miss detection rate is less than 5% in the dugout tunnel of coal mine.

Keywords: Mining Security; Coal safety assessment; Artificial neural network; Transfer learning

1. Introduction

With the rapid improvement of coal mine informationization [1, 2], deep learning recognition technology [3, 4] has drawn considerable attention in underground mining safety assessment. Compared with the traditional miner management system [5, 6], the underground coal mine face recognition system [7] can provide timely, comprehensive and reliable miner identification information to the daily personnel management agencies of the mine, and provide the rescuers with the identity and regional location information of the trapped miners in the event of a mining accident. It plays an important role in curbing underground overcrowding production, strengthening mine management [8] and emergency rescue. However, the environment of underground coal mine not only has poor lighting conditions, but also the coal mining process is accompanied by a large amount

of dust, steam and coal ash, which make face recognition much more difficult in underground coal mine. To this avail, this paper aims to present an optimized face recognition algorithm to improve the accuracy of face recognition system in underground coal mine.

The traditional representation method for obscured face recognition is the sparse representation method. Sparse representation classification [9] (SRC) represents high-dimensional image in a low-dimensional space and expects to use the minimum number of training samples while arriving at the minimum fitting error. He et al. [10] proposed a sparse representation algorithm based on the maximum entropy criterion, which can effectively cope with non-gaussian errors and outliers. Aiming to encode more structure information and discriminative information, Zheng et al. [11] integrated the adaptive learning weights into group sparse representation classifier (GSRC). A nuclear norm based matrix regression (NMR) method was proposed by Chen et al. [12] to alleviate the influence of contiguous occlusion on face recognition problems. However, the ability of traditional face recognition method to extract face features is limited, especially when there is occlusion in the face images, the occlusion features are mixed with normal features, which greatly reduces the effectiveness of face recognition. As a result, it is urgent to improve the accuracy rate of face recognition algorithms.

With the development of deep learning [13, 14], the deepening of the network model has greatly improved its feature extraction capability. Wieczorek et al. [15] proposed a face detection model in risk situations based on lightweight convolution neural network. Combining the two tasks of directly extracting age-invariant features and synthesizing face features, Zhao et al. [16] proposed a deep age-invariant model (AIM) for face recognition in the wild. Based on single end-to-end deep neural network with strong anti-occlusion ability, a novel face recognition method was proposed by Qiu et al. [17] to discover the corrupted features and clean them. Aiming to further mitigate the resolution discrepancy due to the resolution limitations, Gao et al. [18] proposed a hierarchical deep CNN feature set-based representation learning for face recognition. However, the current researches on occluded face recognition mainly focus on the occlusion of specific regions [19-21], including eyes and mouth. Moreover, many studies found that most face recognition models can not achieve best results on all face datasets.

In recent years, the progress of deep learning has greatly promoted the improvement of the adaptability of face recognition model. In order to alleviate the poor generalization of face recognition model, transfer learning [22] is applied to the training process of neural network. Cai et al. [23]

proposed a new generative adversarial network (OA-GAN) for natural face de-occlusion without an occlusion mask to overcome face natural occlusion tasks. For mitigating the negative effects of mask on face recognition, a new method was proposed by Zhang et al. [24] to improve the performance of masked face recognition. Shukla et al. [25] proposed a transfer learning using MobileNet V2 to solve the problem of face masked identification and verification. In order to effectively recognize face image taken in unrestricted environment, Tang et al. [26] proposed a face recognition algorithm based on depth map transfer learning. However, the current public face dataset lacks face samples from coal mine environment. Therefore, it is necessary to produce a miner face dataset to fine-tune the transfer model.

In this paper, an improved face recognition method for underground coal dust occlusion based on transfer learning is proposed to solve the problem of random coal dust obscuration. Firstly, a novel DS-inception block is designed to reduce the amount of model parameters, and this work establishes a multiscale neural network named DSR-inception. Moreover, a joint supervised loss function based on center loss and softmax loss is proposed to adapt to face recognition classification task. In addition, experimental results show that the face recognition performance indexes of the proposed network in the homemade miner face dataset, such as accuracy, recall and F1-score, are superior to those of other classical face recognition models, and transfer model with joint supervised loss function can achieve the higher recognition accuracy. Lastly, the validity of the proposed face recognition algorithm is verified by industrial test in the dugout tunnel of coal mine.

The remainder of this paper is organized as follows. In section 2, the proposed improved algorithm and model architecture are introduced. In section 3, comparative experiments of model transfer strategy are carried out and the effectiveness of the improved algorithm is verified in the self-made miner face dataset. In section 4, a face recognition system is built and occluded face recognition experiment is carried out in underground coal mine. Conclusions and future works are summarized in section 5.

2. The proposed method

2.1 Transfer learning

Transfer learning uses the network trained by related tasks to apply to other tasks, which solves the problem of insufficient generalization ability of traditional machine learning. In the transfer learning, the domain D can be expressed by Equation (1):

$$D = \{x, P(X)\} \quad (1)$$

where x is the feature space, X is the sample data point and $X = \{x_1, x_2, \ldots, x_n\}$, x_i is the feature vector, $P(X)$ is the marginal probability.

The task T can be expressed by Equation (2):

$$T = \{\gamma, P(\gamma \mid X)\} \quad (2)$$

where γ is the feature space and $P(\gamma \mid X)$ is the objective function.

Based on the above two equations, transfer learning can be defined as: utilizing the knowledge of an existing task T_s in an existing domain D_s to solve the learning task T_t in the target domain D_t and achieve a better conditional probability distribution $P(D_t \mid X_T)$ of the target domain.

2.2 Inception block and depthwise seperable convolution

As shown in Appendix 1, inception block [27] is the basic convolutional block in GoogleNet [28], which is expanded in width by splitting the traditional convolutional kernel into different sized convolutional kernels. Inception block is able to split the single size convolutional kernel into convolutional kernels of different sizes, which enables the network to extract the features of the image more fully and take up less computational resources. The feature maps F' obtained after inception block can be mathematically expressed by Equation (3)-(7):

$$F_1 = ReLU(conv(F, k_{1\times1}) + b_1) \quad (3)$$

$$F_2 = ReLU(conv(ReLU(conv(F, k_{1\times1}) + b_{21}), k_{3\times3}) + b_{22}) \quad (4)$$

$$F_3 = ReLU(conv(ReLU(conv(F, k_{1\times1}) + b_{31}), k_{5\times5}) + b_{32}) \quad (5)$$

$$F_4 = ReLU(conv(MaxPool(F, k_{3\times3}), k_{1\times1}) + b_4) \quad (6)$$

$$F' = Concat(F_1, F_2, F_3, F_4) \quad (7)$$

where F_1, F_2, F_3 and F_4 are respectively the feature maps obtained after four branches, $k_{i\times i}$ is the convolution kernels of size $i\times i$, and b_i is the bias.

Depthwise seperable convolution kernel [29] is a combination of two types of convolution kernels, including depthwise convolution kernel and pointwise convolution kernel. When the traditional convolution kernel convolves the image, channel and spatial information of the image are fused together. While depthwise separable convolution isolates the channel information from the spatial information and processes them separately in turn before fusion.

The depthwise seperable convolution is performed by depth and point channel convolution in two steps. In the depthwise convolution part, the convolution operation is performed on each channel of the image, which uses a single-layer planar convolution kernel to obtain the result of the planar

convolution layer. In the pointwise convolution part, the result of the planar convolution layer operation is stitched, and then the convolution calculation is performed on the feature map using a 1×1 point convolution kernel.

The output feature map for conventional convolution assuming stride one and padding can be expressed by Equation (8):

$$G_{k,l,n} = \sum_{i,j,m} K_{i,j,m,n} \cdot F_{k+i-1,l+j-1,m} \tag{8}$$

where G is the output feature map, F is the input feature map, K is the conventional convolution kernel, and the cost of conventional convolutions can be expressed by Equation (9):

$$Cost = D_K \cdot D_K \cdot M \cdot N \cdot D_F \cdot D_F \tag{9}$$

where $D_K \times D_K$ is the spatial dimension of the kernel, M is the number of input channels, N is the number of output channels, and $D_F \times D_F$ is the size of feature map.

The output feature map of depthwise seperable convolution with the same parameters can be expressed by Equation (10):

$$\widehat{G}_{k,l,m} = \sum_{i,j} \widehat{K}_{i,j,m} \cdot F_{k+i-1,l+j-1,m} \tag{10}$$

where $\widehat{G}$ is the output feature map, $\widehat{F}$ is the input feature map, $\widehat{K}$ is the depthwise seperable convolution kernel, and the cost of depthwise seperable convolutions can be expressed by Equation (11):

$$\widehat{Cost} = D_K \cdot D_K \cdot M \cdot D_F \cdot D_F + M \cdot N \cdot D_F \cdot D_F \tag{11}$$

which is the sum of the depthwise convolution and 1 × 1 pointwise convolution. By replacing traditional convolution with depthwise seperable convolution can reduce the size and computational effort of the network model, and the value can be expressed by Equation (12):

$$\frac{\widehat{Cost}}{Cost} = \frac{D_K \cdot D_K \cdot M \cdot D_F \cdot D_F + M \cdot N \cdot D_F \cdot D_F}{D_K \cdot D_K \cdot M \cdot N \cdot D_F \cdot D_F} = \frac{1}{N} + \frac{1}{{D_K}^2} \tag{12}$$

2.3 Improved DS-Inception block

In this paper, the depthwise seperable convolution is fused into the inception block, and the traditional convolution kernel is replaced by the depthwise seperable convolution kernel. The improved convolution block is called as DS-Inception, and the specific design structure is shown in Appendix 2. The feature maps F' obtained after DS-Inception block can be mathematically expressed by Equation (13)-(18):

$$F_1 = ReLU(conv(F, k_{1\times1}) + b_1) \tag{13}$$

$$F_2 = ReLU(Dw(ReLU(conv(F, k_{1\times1}) + b_2), k_{3\times3})) \tag{14}$$

$$F_3 = ReLU(Dw(ReLU(conv(F, k_{1\times1}) + b_3), k_{5\times5})) \tag{15}$$

$$F_4 = ReLU(conv(MaxPool(F, k_{3\times3}), k_{1\times1}) + b_4) \tag{16}$$

$$F_5 = ReLU(conv(F, k_{1\times1}) + b_5) \tag{17}$$

$$F' = Add(Concat(F_1, F_2, F_3, F_4), F_5) \tag{18}$$

where F_1, F_2, F_3, F_4 and F_5 are respectively the feature maps obtained from the five branches, $k_{i\times i}$ is the convolution kernels of size $i\times i$, and b_i is the bias.

The depthwise seperable convolution substitution is carried out for the large convolution kernel in inception block, and the residual structure is introduced into this block. Many studies have shown that the residual structure [30] can effectively restrain the gradient dispersion of the network and accelerate the convergence speed of the model. The parameters of the improved inception block are greatly reduced compared with the original structure block. The number of channels of each branch convolution kernel is K and the number of channels of the input layer is N; so, the number of parameters of the original block is $4NK + 34K^2$ and the number for the improved block is $4NK + 34K + 2K^2$, which is $32K^2 - 34K$ fewer than the original block.

2.4 Improved multiscale neural network

In this paper, referring to VGG-16 architecture, a multiscale convolutional neural network model based on the DS-Inception block is designed, called as DSR-inception network (see Figure 1). The proposed network mainly includes pooling module and convolution module which consists of DS-inception block, relu activation function and batch normalization. The five traditional convolutional modules of VGG-16 are replaced with the proposed convolutional modules to significantly reduce the number of model parameters. The ReLU activation function is assigned to neurons in all convolutional and fully connected layer, whereas the Sigmoid activation function is applied to neurons in the last layer for outputting the classification results. There is a max-pooling layer with a size of 2×2 and a stride of 2 behind each continuous convolutional layer to aggregate the transmitted information. The number of filters in the network increases as its depth increases, allowing for the learning of more detailed information from the input image.

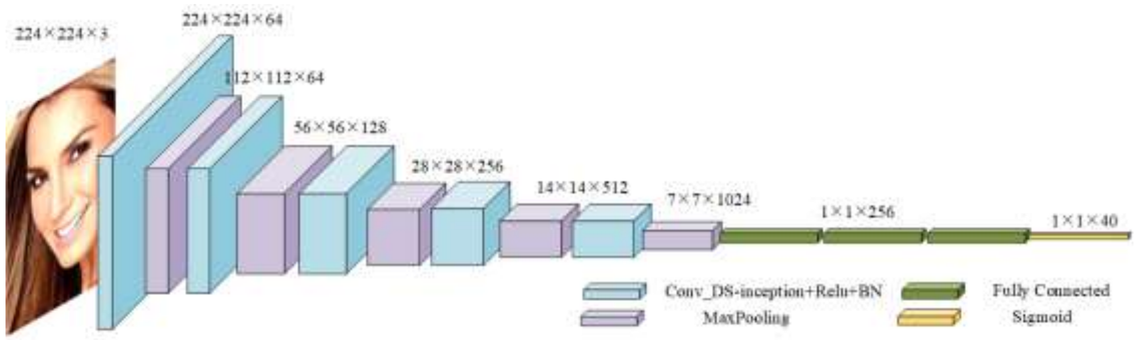

Figure 1. Framework of DSR-Inception network.

As it is the processing flow of the designed network model is illustrated in Figure 2. First, the face image of size 224×224×3 is input to the network through two branches. One branch passes through DS-inception block, each branch of this convolution block uses 16 convolution kernels for convolution operation. After passing through the module, the feature map of size 224×224×64 is output. The other branch adjusts the number of channels through the residual block. The corresponding element values of the feature map of the two branches are summed, and then the feature map is input into relu activation function, batch normalization and pooling layer. After five times of the above operation, the face features in the image are fully extracted, and the feature map of size 7×7×1024 is obtained. Next, the feature map is input into global average pooling layer and dropout layer, and recognized result is output by the sigmoid classifier.

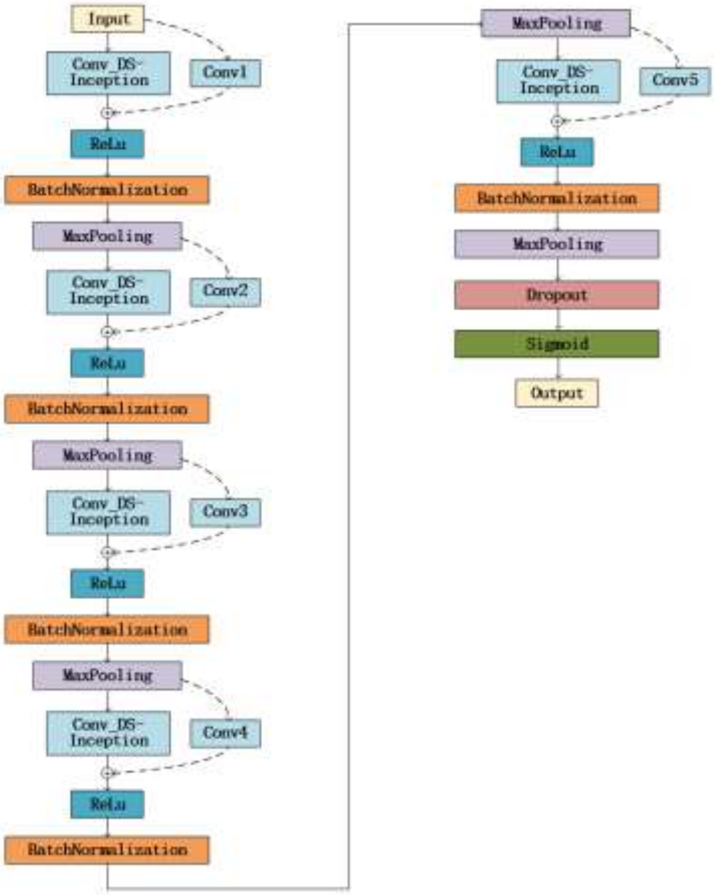

Figure 2. Processing flow of DSR-Inception network.

The designed multiscale neural network contains convolutional kernels of different sizes to extract features of different dimensions, so the problem about low accuracy in facial feature extracted with a single scale network can be solved. Moreover, the residual structure is added to accelerate the convergence speed of network training and prevent overfitting.

2.5 Joint supervised loss function

The essence of the optimization process in the classification problem is the process of

minimizing the objective function. Softmax loss function is commonly used in the problem of image multiclassification, which is defined as shown in Equation (19) below.

$$L_s = -\frac{1}{m}\sum_{i=1}^{m}\log\frac{e^{W_{y_i}^T x_i + b_{yi}}}{\sum_{j=1}^{n} e^{W_{y_i}^T x_i + b_{yi}}} \tag{19}$$

Softmax loss function has good differentiability but lacks discriminative power. The redundancy of inter-class features is high in face recognition tasks, and it may lead to a greater difference between faces of the same person.

Center loss function [31] is a clustering algorithm that causes each class to cluster to a center, which is equivalent to attaching a strong constraint to each class. It is defined in Equation (20).

$$L_c = \frac{1}{2}\sum_{i=1}^{m}\left\|x_i - c_{yi}\right\|_2^2 \tag{20}$$

The joint supervised loss function consists of softmax loss function and center loss function, which is a powerful tool used in facial recognition technology for optimizing classification accuracy and feature center clustering simultaneously, and the schematic of the function is shown in Appendix 3. The softmax loss function aims to maximize the accuracy of face classification by minimizing the difference between the model's output probability distribution and the true label. On the other hand, the center loss function seeks to cluster feature vectors of the same category close to a center point while separating those of different categories to enhance the identification of identity information. Furthermore, the center loss function incorporates a weight parameter λ, which helps regulate the influence and update speed of the center point. Equation (21) shows the joint supervised loss function.

$$L = L_s + \lambda L_c = -\sum_{i=1}^{m}\log\frac{e^{W_{yi}^T xi + b_{yi}}}{\sum_{j=1}^{n} e^{W_{yi}^T xi + b_{yi}}} + \frac{\lambda}{2}\sum_{i=1}^{m}\left\|x_i - c_{yi}\right\|_2^2 \tag{21}$$

where m, n are respectively the number of samples and categories, x_i is the feature of image, y_i is the label of category, W_j is the weight of fully connected layer, b is the bias, c_{yi} is the center of the classification, λ is the equilibrium coefficient and $\lambda \in (0, 0.1)$, and the value of λ is 0.01 in this paper.

3. Experimental results and analysis

3.1 Experimental platform

The model is trained in the GPU environment, and the environment configuration is shown in Table 1 beow.

Table 1. Training environment configuration.

Name	Parameter

CPU	Intel Core i9-10980XE
Hard Disc	2T
GPU	NVIDIA RTX A4000
Memory	16G
Deep learning framework	TensorFlow2.6.0
Operating system	Window10
Programming language	Python3.7
Cuda	10.0

3.2 Dataset

The pre-training dataset selected in this paper is the CelebA face dataset, the face data in this dataset is given in terms of face attributes for classification, and each face picture is given with face frame marker points. Appendix 4 shows a protion of the face images in the dataset.

The homemade miner face dataset is named MF dataset. The MF dataset contains 40 people with 21 pictures each, including 7 pictures each of no coal ash obscuration, light coal ash obscuration and heavy coal ash obscuration, for a total of 840 pictures. Table 2 shows an example of face data for the same person.

Table 2. Sample face data from the same person.

Attribute	front 0^0	right 15^0	right 45^0	left 15^0	left 45^0	up 15^0	down 15^0
without obscuration							
light obscuration							
heavy obscuration							

3.3 Contrast experiment

In this paper, stochastic gradient descent (SGD) is chosen as the optimizer of training, the remaining hyperparameters, including batch size, initial learning rate a_0, natural decay index β and epoch, are set to 64, 0.01, 0.05 and 150, respectively. Inceptionv1, VGG-16 and Resnet18 are selected as the comparison network models and trained on the CelebA face dataset. The accuracy and loss of models during training are shown in Appendix 5, which shows that the proposed DSR-inception network has better advantages in terms of convergence speed and correctness compared with other network models.

Table 3. Design of different transfer learning schemes.

Number	Transfer strategy	Train sample	Test sample
a	without retraining	14000	4000
b	freeze the weight of Conv1 and retrain the rest		
c	freeze the weight of Conv1~2 and retrain the rest		
d	freeze the weight of Conv1~3 and retrain the rest		
e	freeze the weight of Conv1~4 and retrain the rest		
f	freeze the weight of all convolution layer		

The specific transfer strategy is shown in Table 3 and the comparison data after the experiments are shown in Appendix 6. The effect of transfer learning is best when the module weights of Conv1~3 are frozen and the rest are retrained.

The CelebA face dataset is selected for model pre-training, of which 14,000 are used for training and 4,000 are used for testing. The specific experimental results are shown in Table 4. It can be seen that the proposed model has a higher accuracy and recall rate than other network models. Moreover, the size of the proposed model is only 46.56M, and the average time spent for testing each face image is 258ms.

Table 4. Experimental comparison of different network.

Metrics Model	Precision	Recall	F1-score	Memory (M)	Test time (ms/pic)
Inceptionv1	95.34%	90.86%	93.05%	189	547
VGG-16	91.53%	88.39%	89.93%	526	625
Resnet18	94.82%	89.73%	92.21%	246	443
Proposed	**97.26%**	**94.17%**	**95.42%**	**46.56**	**258**

The MF dataset is selected for model fine-tuning, and introducing the improved loss function as a variable is tested for comparison. The experimental results are shown in Appendix 7. From the average results of 20 groups of experiments, it can be seen that the F1-score of the model with joint supervised loss function is about 0.5%~1.5% higher than before, which verifies the effectiveness of joint supervised loss function.

This paper also compared the proposed model with some new mainstream methods on CelebA face dataset, and the experimental results are shown in Table 5.

Table 5 Comparison between proposed model and state-of-the-art methods.

Model	Accuracy (%)
SNNBFR **[32]**	93.54

OPFaceNet **[33]**	96.83
IFDM **[34]**	95.64
LSCSR **[35]**	96.50
MFR **[36]**	96.78
MMPCANet **[37]**	97.18
Proposed	**97.26**

As can be seen from Table 5, the performance of the method presented in this paper exceeds that of most existing methods. Compared with the other methods, the detection accuracy of the proposed method is higher, indicating that the detection accuracy of the occluded face can be improved effectively by fusing the multi-scale features of the face.

4. Application of proposed approach in underground coal mine

In order to further verify the feasibility of the proposed face recognition system in underground coal mines, the face recognition system is set up in the tunneling tunnel. The mining monitoring camera KBA18W is selected to obtain images, and the signal is transmitted through the underground wireless router. The LED light source is used as auxiliary lighting equipment and the industrial test site equipment is set up as shown in Figure 3(a).

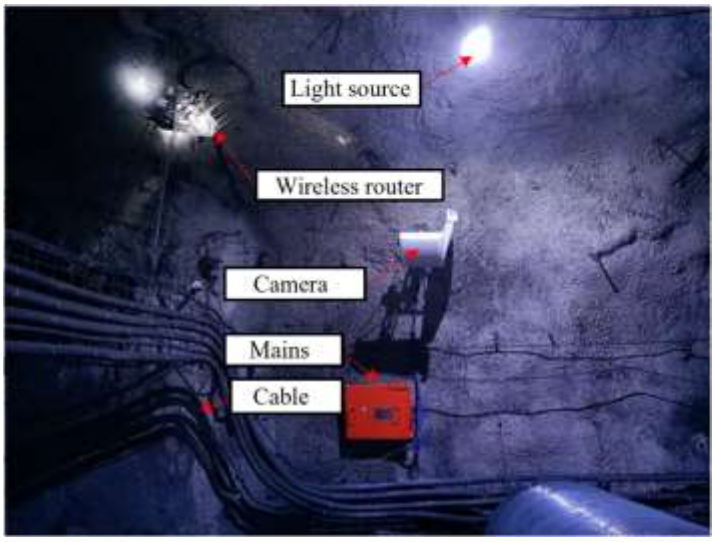

(a) Industrial test scene

(b) Running interface of face recognition system

Figure 3. Field testing.

Before the industrial test, the face data of the staff members, a total of 6 people, is registered into the system. The system display interface is shown in Figure 3(b).

A 60-hour working period is selected to verify the feasibility of the system, and the recognition results of the face recognition system are counted to verify the recognition rate of the system. The system recognition results are shown in Table 6.

Table 6. Industrial test result.

	XW-01	XW-02	XW-03	XW-04	XW-05	XW-06	Average
Number of faces	296	320	453	416	380	374	-
Precision	89.73%	90.94%	91.34%	92.86%	91.04%	92.16%	91.34%
Loss	6.42%	4.84%	3.81%	3.57%	3.92%	3.12%	4.28%

The average recognition accuracy of the proposed face recognition system in the dugout tunnel of coal mine reaches 91.34% and the miss detection rate is less than 5%. The results of the industrial test show that the system meets the design requirements.

5. Conclusions and future work

In this paper, an improved face recognition method for underground coal mine based on transfer learning is proposed to solve the problem of random coal dust obscuration. A novel DS-inception block is designed to reduce the amount of model parameters, and a joint supervised loss function based on center loss and softmax loss is proposed to adapt to face recognition classification task. Compared with the other classical models such as Inceptionv1, VGG-16 and Resnet-18, the various evaluation indicators of the proposed multiscale neural network, including accuracy, recall and F1-

score, achieve 97.26%, 94.17% and 95.42%, respectively. In order to better adapt to the face recognition task in coal mine, a miner face dataset is made to fine-tune the transfer model, and the transfer model incorporating joint supervised loss can effectively improve the face recognition accuracy by about 0.5~1.5%. In addition, the average recognition accuracy of the designed face recognition system in the dugout tunnel of coal mine reaches 91.34%, and the miss detection rate is less than 5%.

This paper verifies the effectiveness of the proposed face recognition method in underground coal mine. However, this work has not yet considered the face recognition under the change of large angle posture, and further research on face recognition under different postures is needed in the future.

Acknowledgements

The research leading to these results has received funding from the Norwegian Financial Mechanism 2014-2021 under Project Contract No 2020/37/K/ST8/02748.

Conflict of interests

The authors declare that there is no conflict of interests regarding the publication of this article.

Data Availability

All data that produce the results in this work can be requested from the corresponding author.

References

[1] X. P. Yuan, "Development of the large-scale coal base and the modern mine in China: The present situation and future tasks," in *1st International Conference on Energy and Environmental Protection (ICEEP 2012)*, Hohhot, PEOPLES R CHINA, Jun 23-24 2012, vol. 524-527, in Advanced Materials Research, 2012, pp. 3066-3069, doi: 10.4028/www.scientific.net/AMR.524-527.3066. [Online]. Available: <Go to ISI>://WOS:000313544101199

[2] A. X. Zhao, "The Analysis of Coal Safety Production Monitoring Data Based on Deep Learning," in *13th International Conference on Natural Computation, Fuzzy Systems and Knowledge Discovery (ICNC-FSKD)*, Guilin, PEOPLES R CHINA, Jul 29-31 2017, 2017, pp. 1053-1057. [Online]. Available: <Go to ISI>://WOS:000437355301017. [Online]. Available: <Go to ISI>://WOS:000437355301017

[3] Z. Y. Liu, A. Wang, and L. Li, "DEEP LEARNING OF UNDERGROUND COGNITIVE RADIO MODULATION RECOGNITION TECHNOLOGY USING FOR COAL MINING," *Fresenius Environmental Bulletin,* vol. 31, no. 10, pp. 9890-9900, 2022. [Online]. Available: <Go to ISI>://WOS:000883305600001.

[4] X. C. Guo, M. Liu, and D. E. P. Inc, "Research on the Face Image Detection in Coal Mine Environment," in *International Conference on Electronic, Information Technology and*

Intellectualization (ICEITI), Guangzhou, PEOPLES R CHINA, Jun 18-19 2016, 2016, pp. 375-379. [Online]. Available: <Go to ISI>://WOS:000385265600055. [Online]. Available: <Go to ISI>://WOS:000385265600055

[5] Y. F. Li, H. J. Chen, and J. P. Li, "STUDY ON INFORMATION MANAGEMENT SYSTEM AND ITS APPLICATION IN COLLIERY ENTERPRISES," in *13th International Conference on Enterprise Information Systems (ICEIS 2011)*, Beijing Jiaotong Univ, Sch Econ & Management, Beijing, PEOPLES R CHINA, Jun 08-11 2011, 2011, pp. 589-592. [Online]. Available: <Go to ISI>://WOS:000393449200089. [Online]. Available: <Go to ISI>://WOS:000393449200089

[6] Q. Zhang, "RFID-Based Coal Mine Personnel Management System Development," in *International Conference on Energy, Environment and Materials Engineering (EEME)*, Shenzhen, PEOPLES R CHINA, Feb 22-23 2014, 2014, pp. 962-965. [Online]. Available: <Go to ISI>://WOS:000351909800181. [Online]. Available: <Go to ISI>://WOS:000351909800181

[7] H. Yang and X. F. Han, "Face Recognition Attendance System Based on Real-Time Video Processing," *Ieee Access,* vol. 8, pp. 159143-159150, 2020, doi: 10.1109/access.2020.3007205.

[8] K. Yu, L. J. Zhou, P. P. Liu, J. Chen, D. J. Miao, and J. S. Wang, "Research on a Risk Early Warning Mathematical Model Based on Data Mining in China's Coal Mine Management," *Mathematics,* vol. 10, no. 21, Nov 2022, Art no. 4028, doi: 10.3390/math10214028.

[9] J. Wright, A. Y. Yang, A. Ganesh, S. S. Sastry, and Y. Ma, "Robust Face Recognition via Sparse Representation," *Ieee Transactions on Pattern Analysis and Machine Intelligence,* vol. 31, no. 2, pp. 210-227, Feb 2009, doi: 10.1109/tpami.2008.79.

[10] R. He, W. S. Zheng, and B. G. Hu, "Maximum Correntropy Criterion for Robust Face Recognition," *Ieee Transactions on Pattern Analysis and Machine Intelligence,* vol. 33, no. 8, pp. 1561-1576, Aug 2011, doi: 10.1109/tpami.2010.220.

[11] J. W. Zheng, P. Yang, S. Y. Chen, G. J. Shen, and W. L. Wang, "Iterative Re-Constrained Group Sparse Face Recognition With Adaptive Weights Learning," *Ieee Transactions on Image Processing,* vol. 26, no. 5, pp. 2408-2423, May 2017, doi: 10.1109/tip.2017.2681841.

[12] Z. Chen, X. J. Wu, and J. Kittler, "A sparse regularized nuclear norm based matrix regression for face recognition with contiguous occlusion," *Pattern Recognition Letters,* vol. 125, pp. 494-499, Jul 2019, doi: 10.1016/j.patrec.2019.05.018.

[13] K. M. He, X. Y. Zhang, S. Q. Ren, J. Sun, and Ieee, "Deep Residual Learning for Image Recognition," in *2016 IEEE Conference on Computer Vision and Pattern Recognition (CVPR)*, Seattle, WA, Jun 27-30 2016, in IEEE Conference on Computer Vision and Pattern Recognition, 2016, pp. 770-778, doi: 10.1109/cvpr.2016.90. [Online]. Available: <Go to ISI>://WOS:000400012300083

[14] M. Ye, J. B. Shen, G. J. Lin, T. Xiang, L. Shao, and S. C. H. Hoi, "Deep Learning for Person Re-Identification: A Survey and Outlook," *Ieee Transactions on Pattern Analysis and Machine Intelligence,* vol. 44, no. 6, pp. 2872-2893, Jun 2022, doi: 10.1109/tpami.2021.3054775.

[15] M. Wieczorek, J. Silka, M. Wozniak, S. Garg, and M. M. Hassan, "Lightweight Convolutional Neural Network Model for Human Face Detection in Risk Situations," *Ieee Transactions on Industrial Informatics,* vol. 18, no. 7, pp. 4820-4829, Jul 2022, doi: 10.1109/tii.2021.3129629.

[16] J. Zhao, S. C. Yan, and J. S. Feng, "Towards Age-Invariant Face Recognition," *Ieee Transactions on Pattern Analysis and Machine Intelligence,* vol. 44, no. 1, pp. 474-487, Jan

2022, doi: 10.1109/tpami.2020.3011426.

[17] H. B. Qiu, D. H. Gong, Z. F. Li, W. Liu, and D. C. Tao, "End2End Occluded Face Recognition by Masking Corrupted Features," *Ieee Transactions on Pattern Analysis and Machine Intelligence,* vol. 44, no. 10, pp. 6939-6952, Oct 2022, doi: 10.1109/tpami.2021.3098962.

[18] G. W. Gao, Y. Yu, J. Yang, G. J. Qi, and M. Yang, "Hierarchical Deep CNN Feature Set-Based Representation Learning for Robust Cross-Resolution Face Recognition," *Ieee Transactions on Circuits and Systems for Video Technology,* vol. 32, no. 5, pp. 2550-2560, May 2022, doi: 10.1109/tcsvt.2020.3042178.

[19] Y. Li, J. B. Zeng, S. G. Shan, and X. L. Chen, "Occlusion Aware Facial Expression Recognition Using CNN With Attention Mechanism," *Ieee Transactions on Image Processing,* vol. 28, no. 5, pp. 2439-2450, May 2019, doi: 10.1109/tip.2018.2886767.

[20] D. Zeng, R. Veldhuis, and L. Spreeuwers, "A survey of face recognition techniques under occlusion," *Iet Biometrics,* vol. 10, no. 6, pp. 581-606, Nov 2021, doi: 10.1049/bme2.12029.

[21] A. Alzu'bi, F. Albalas, T. Al-Hadhrami, L. B. Younis, and A. Bashayreh, "Masked Face Recognition Using Deep Learning: A Review," *Electronics,* vol. 10, no. 21, Nov 2021, Art no. 2666, doi: 10.3390/electronics10212666.

[22] F. Z. Zhuang *et al.*, "A Comprehensive Survey on Transfer Learning," *Proceedings of the Ieee,* vol. 109, no. 1, pp. 43-76, Jan 2021, doi: 10.1109/jproc.2020.3004555.

[23] J. C. Cai, H. Han, J. Y. Cui, J. Chen, L. Liu, and S. K. Zhou, "Semi-Supervised Natural Face De-Occlusion," *Ieee Transactions on Information Forensics and Security,* vol. 16, pp. 1044-1057, 2021, doi: 10.1109/tifs.2020.3023793.

[24] M. Zhang, R. J. Liu, D. Deguchi, and H. Murase, "Masked Face Recognition With Mask Transfer and Self-Attention Under the COVID-19 Pandemic," *Ieee Access,* vol. 10, pp. 20527-20538, 2022, doi: 10.1109/access.2022.3150345.

[25] R. K. Shukla and A. K. Tiwari, "Masked Face Recognition Using MobileNet V2 with Transfer Learning," *Computer Systems Science and Engineering,* vol. 45, no. 1, pp. 293-309, 2023, doi: 10.32604/csse.2023.027986.

[26] D. J. Tang and J. L. Hao, "A deep map transfer learning method for face recognition in an unrestricted smart city environment," *Sustainable Energy Technologies and Assessments,* vol. 52, Aug 2022, Art no. 102207, doi: 10.1016/j.seta.2022.102207.

[27] X. Jin *et al.*, "Deep Image Aesthetics Classification using Inception Modules and Fine-tuning Connected Layer," in *8th International Conference on Wireless Communications and Signal Processing (WCSP)*, Yangzhou, PEOPLES R CHINA, Oct 13-15 2016, in International Conference on Wireless Communications and Signal Processing, 2016. [Online]. Available: <Go to ISI>://WOS:000391540800129. [Online]. Available: <Go to ISI>://WOS:000391540800129

[28] J. W. Li, G. Song, and M. H. Zhang, "Occluded offline handwritten Chinese character recognition using deep convolutional generative adversarial network and improved GoogLeNet," *Neural Computing & Applications,* vol. 32, no. 9, pp. 4805-4819, May 2020, doi: 10.1007/s00521-018-3854-x.

[29] J. H. Wei, Y. Zhou, W. Xie, J. W. Yu, W. S. Li, and Ieee, "Compression algorithm for live face recognition model based on depth-separable convolution," in *33rd Chinese Control and Decision Conference (CCDC)*, Kunming, PEOPLES R CHINA, May 22-24 2021, in Chinese Control and Decision Conference, 2021, pp. 1624-1628, doi: 10.1109/ccdc52312.2021.9602667. [Online]. Available: <Go to ISI>://WOS:000824370101149

[30] H. L. Yu *et al.*, "Apple leaf disease recognition method with improved residual network," *Multimedia Tools and Applications,* vol. 81, no. 6, pp. 7759-7782, Mar 2022, doi: 10.1007/s11042-022-11915-2.
[31] Z. J. Hu *et al.*, "Dual Distance Center Loss: The Improved Center Loss That Can Run Without the Combination of Softmax Loss, an Application for Vehicle Re-Identification and Person Re-Identification," *Ieee Transactions on Computational Social Systems,* vol. 9, no. 5, pp. 1345-1358, Oct 2022, doi: 10.1109/tcss.2021.3127561.
[32] R. Chatterjee, S. Roy, and S. Roy, "A Siamese Neural Network-Based Face Recognition from Masked Faces," in *1st International Conference on Advanced Network Technologies and Intelligent Computing (ANTIC)*, Electr Network, Dec 17-18 2021, vol. 1534, in Communications in Computer and Information Science, 2022, pp. 517-529, doi: 10.1007/978-3-030-96040-7_40. [Online]. Available: <Go to ISI>://WOS:000772182600040
[33] G. Lokku, G. H. Reddy, and M. N. G. Prasad, "OPFaceNet: OPtimized Face Recognition Network for noise and occlusion affected face images using Hyperparameters tuned Convolutional Neural Network," *Applied Soft Computing,* vol. 117, Mar 2022, Art no. 108365, doi: 10.1016/j.asoc.2021.108365.
[34] D. Mamieva, A. B. Abdusalomov, M. Mukhiddinov, and T. K. Whangbo, "Improved Face Detection Method via Learning Small Faces on Hard Images Based on a Deep Learning Approach," *Sensors,* vol. 23, no. 1, Jan 2023, Art no. 502, doi: 10.3390/s23010502.
[35] J. X. Mi, Q. Huang, and L. F. Zhou, "Local spatial continuity steered sparse representation for occluded face recognition," *Multimedia Tools and Applications,* vol. 81, no. 18, pp. 25147-25170, Jul 2022, doi: 10.1007/s11042-022-12427-9.
[36] S. Mishra and H. Reza, "A Face Recognition Method Using Deep Learning to Identify Mask and Unmask Objects," in *IEEE World AI IoT Congress (AIIoT)*, Seattle, WA, Jun 06-09 2022, 2022, pp. 91-99, doi: 10.1109/aiiot54504.2022.9817324. [Online]. Available: <Go to ISI>://WOS:000848394800015
[37] Z. W. Wang, Y. J. Zhang, C. C. Pan, and Z. W. Cui, "MMPCANet: An Improved PCANet for Occluded Face Recognition," *Applied Sciences-Basel,* vol. 12, no. 6, Mar 2022, Art no. 3144, doi: 10.3390/app12063144.